

Thermodynamics of frustrated ferromagnetic spin-1/2 Heisenberg chains: The role of inter-chain coupling

P. Müller and J. Richter

Institut für Theoretische Physik, Otto-von-Guericke-Universität Magdeburg, D-39016 Magdeburg, Germany

D. Ihle

Institut für Theoretische Physik, Universität Leipzig, D-04109 Leipzig, Germany

(Dated: March 16, 2017)

The thermodynamics of coupled frustrated ferromagnetic chains is studied within a spin-rotation-invariant Green's function approach. We consider an isotropic Heisenberg spin-half system with a ferromagnetic in-chain coupling $J_1 < 0$ between nearest neighbors and a frustrating antiferromagnetic next-nearest neighbor in-chain coupling $J_2 > 0$. We focus on moderate strength of frustration $J_2 < |J_1|/4$ such that the in-chain spin-spin correlations are predominantly ferromagnetic. We consider two inter-chain couplings (ICs) $J_{\perp,y}$ and $J_{\perp,z}$, corresponding to the two axis perpendicular to the chain, where ferromagnetic as well as antiferromagnetic ICs are taken into account. We discuss the influence of frustration on the ground-state properties for antiferromagnetic ICs, where the ground state is of quantum nature. The major part of our study is devoted to the finite-temperature properties. We calculate the critical temperature T_c as a function of the competing exchange couplings $J_2, J_{\perp,y}, J_{\perp,z}$. We find that for fixed ICs T_c monotonically decreases with increasing frustration J_2 , where as $J_2 \rightarrow |J_1|/4$ the $T_c(J_2)$ -curve drops down rapidly. To characterize the magnetic ordering below and above T_c we calculate the spin-spin correlation functions $\langle \mathbf{S}_0 \mathbf{S}_{\mathbf{R}} \rangle$, the magnetic order parameter M , the uniform static susceptibility χ_0 as well as the correlation length ξ . Moreover, we discuss the specific heat C_V and the temperature dependence of the excitation spectrum $\omega_{\mathbf{q}}$. As $J_2 \rightarrow |J_1|/4$ some unusual frustration-induced features were found, such as an increase of the in-chain spin stiffness (in case of ferromagnetic ICs) or of the in-chain spin-wave velocity (in case of antiferromagnetic ICs) with growing temperature.

I. INTRODUCTION

One-dimensional (1D) frustrated quantum J_1 - J_2 Heisenberg systems have been studied intensively for many years.^{1–29} They exhibit a large variety of physical many-body phenomena. Many experimental studies have shown that there is a plethora of materials, such as the edge-shared cuprates LiVCuO_4 , LiCu_2O_2 , NaCu_2O_2 , $\text{Li}_2\text{ZrCuO}_4$, $\text{Ca}_2\text{Y}_2\text{Cu}_5\text{O}_{10}$, and Li_2CuO_2 , which can be adequately described by a chain model with ferromagnetic (FM) nearest neighbors (NN) interaction J_1 and antiferromagnetic (AFM) next-nearest neighbors (NNN) interaction J_2 .^{30–48}

From the experimental point of view it is clear that an inter-chain coupling (IC) is unavoidably present in real materials, that leads to three-dimensional (3D) physics at least at low temperatures, and, in particular, it may lead to a phase transition to a magnetically long-range ordered phase below a critical temperature T_c . Thus, for example, in Refs. 45, 46, and 48 for the magnetic-chain material $\text{Ca}_2\text{Y}_2\text{Cu}_5\text{O}_{10}$ the following parameters were reported $J_1 \approx -93$ K (FM), $J_2 \approx 4.7$ K (AFM), and $T_c \approx 30$ K, indicating the presence of a non-negligible IC. The discussion of the role of the IC makes the theoretical treatment more challenging, since several tools, such as the Density-Matrix Renormalization Group (DMRG) and the Exact Diagonalization (ED), are less effective in dimension $D > 1$. In fact, coupled frustrated spin-chains are much less investigated in literature. Moreover, most of these investigations were focused on ground state (GS)

properties.^{11,15,26,52–55}

In our paper we want to discuss the role of the IC in coupled frustrated spin-1/2 chain magnets with a FM NN in-chain coupling $J_1 < 0$ and an AFM NNN in-chain coupling $J_2 > 0$. According to Fig. 1 the chains are aligned along the x -axis, and they are coupled along the y - and z -axis by $J_{\perp,y}$ and $J_{\perp,z}$, respectively. The two NN ICs $J_{\perp,y}$ and $J_{\perp,z}$ are treated as independent variables which can be FM as well as AFM. The corresponding model reads

$$H = J_1 \sum_{\langle i,j \rangle, x} \mathbf{S}_i \cdot \mathbf{S}_j + J_2 \sum_{[i,j], x} \mathbf{S}_i \cdot \mathbf{S}_j + J_{\perp,y} \sum_{\langle i,j \rangle, y} \mathbf{S}_i \cdot \mathbf{S}_j + J_{\perp,z} \sum_{\langle i,j \rangle, z} \mathbf{S}_i \cdot \mathbf{S}_j, \quad (1)$$

where $\langle i, j \rangle, x, y, z$ labels NN bonds along the corresponding axis and $[i, j], x$ labels NNN bonds along the chain. Moreover, we consider $J_1 < 0$ and $J_2 \geq 0$, whereas no sign restrictions are valid for $J_{\perp,y}$ and $J_{\perp,z}$.

An appropriate method to study thermodynamic properties of the model (1) in the whole temperature range is the second-order rotation-invariant Green's function method, see, e.g., Refs. 9, 19, 20, 56–70. This method has been used recently for the 1D J_1 - J_2 model,^{9,19} for the frustrated square-lattice ferromagnet⁶⁹ as well as for the 3D frustrated ferromagnet on the body-centered cubic lattice.⁷⁰

For the classical model (1) in $D = 1$ (i.e., $s \rightarrow \infty$ and $J_{\perp,y} = J_{\perp,z} = 0$) the critical strength of frustration, where the FM GS breaks down, is $J_2^{c, \text{clas}} = |J_1|/4$,

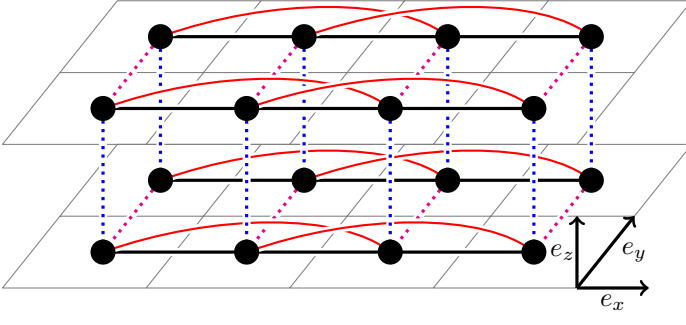


Figure 1. (Color online) Sketch of the considered model of coupled frustrated spin chains: J_1 - NN in-chain coupling (solid black), J_2 - NNN in-chain coupling (solid red), $J_{\perp,y}$ - NN inter-chain coupling in y -direction (dotted magenta), $J_{\perp,z}$ - NN inter-chain coupling in z -direction (dotted blue).

which is also the quantum-critical point J_2^c for the spin-1/2 model.² For $J_2 < J_2^c$ the GS is FM, whereas for $J_2 > J_2^c$ the GS is a quantum spin singlet with incommensurate spiral correlations.^{2,3,5,6} On the classical level, the spiral phase does not depend on the IC couplings $J_{\perp,y}$, or $J_{\perp,z}$ respectively, whereas for the quantum model the spiral phase does depend on the IC coupling, see, e.g., Refs. 11 and 55.

In the present paper we will focus on the parameter region of weak frustration $J_2 < J_2^c$. Although, for those values of J_2 the GS is FM (i.e. it is a classical state without quantum fluctuations), the frustrating NNN bond J_2 may influence the thermodynamics substantially, in particular in the vicinity of the zero-temperature transition, i.e., at $J_2 \lesssim J_2^c$.^{9,19,69-71}

We mention here that the case of coupled AFM spin-1/2 Heisenberg chains is well studied, see, e.g., Refs. 72-75. Since in this case the GS of the isolated chain is of quantum nature and does not exhibit magnetic long-range order the behavior for small IC is different to our case of FM chains.

It is appropriate to notice that in real edge-shared cuprates often the inter-chain coupling is more sophisticated than that we consider in our paper. Moreover, there is a large variety in the topology of the IC, see, e.g., Ref. 54. However, the simplest case of a perpendicular IC J_{\perp} corresponds, e.g., to LiVCuO₄ and Li(Na)Cu₂O₂.^{30,31,34,47} Furthermore, we note that most of these compounds exhibit spiral spin-spin correlations along the chain direction, i.e., the frustration exceeds J_2^c . Hence, there is no direct relation of our results to those compounds with $J_2 > J_2^c$, and the focus here is on the general question for the crossover from a purely 1D $J_1 - J_2$ ferromagnet to a quasi-1D and finally to a 3D system.

II. ROTATION-INVARIANT GREEN'S FUNCTION METHOD (RGM)

The RGM has been widely applied to frustrated quantum spin systems.^{9,19,20,60,62-64,67-70} Therefore, we illustrate here only some basic relevant features of the method. At that we follow Refs. 9 and 70. The retarded two-time Green's function in momentum space $\langle\langle S_{\mathbf{q}}^+; S_{-\mathbf{q}}^- \rangle\rangle_{\omega} = -\chi_{\mathbf{q}}^{+-}(\omega)$ determines the spin-spin correlation functions and the thermodynamic quantities. The equation of motion in the second order using spin rotational symmetry, i.e., $\langle S_i^z \rangle = 0$, is expressed as $\omega^2 \langle\langle S_{\mathbf{q}}^+; S_{-\mathbf{q}}^- \rangle\rangle_{\omega} = M_{\mathbf{q}} + \langle\langle -\ddot{S}_{\mathbf{q}}^+; S_{-\mathbf{q}}^- \rangle\rangle_{\omega}$ with $M_{\mathbf{q}} = \langle\langle [S_{\mathbf{q}}^+, H], S_{-\mathbf{q}}^- \rangle\rangle$ and $-\ddot{S}_{\mathbf{q}}^+ = \langle\langle [S_{\mathbf{q}}^+, H], H \rangle\rangle$. For our model (1) the moment $M_{\mathbf{q}}$ is given by

$$M_{\mathbf{q}} = 4J_1 c_{100}(\cos(q_x) - 1) + 4J_2 c_{200}(\cos(2q_x) - 1) + 4J_{\perp,y} c_{010}(\cos(q_y) - 1) + 4J_{\perp,z} c_{001}(\cos(q_z) - 1), \quad (2)$$

where $c_{hkl} \equiv c_{\mathbf{R}} = \langle S_0^+ S_{\mathbf{R}}^- \rangle = 2\langle S_0 S_{\mathbf{R}} \rangle / 3$, $\mathbf{R} = h\mathbf{a}_1 + k\mathbf{a}_2 + l\mathbf{a}_3$, (\mathbf{a}_j are the cartesian unit vectors). For the second derivative $-\ddot{S}_i^+$ we apply the decoupling scheme in real space⁵⁶⁻⁶²

$$S_i^+ S_j^+ S_k^- = \alpha_{i,k} \langle S_i^+ S_k^- \rangle S_j^+ + \alpha_{j,k} \langle S_j^+ S_k^- \rangle S_i^+, \quad (3)$$

where $i \neq j \neq k \neq i$ and the quantities $\alpha_{i,j}$ are vertex parameters introduced to improve the decoupling approximation. In the minimal version of the RGM we consider as many vertex parameters as independent conditions for them can be found, i.e., we have α_x , α_y , and α_z , related to in-chain (α_x) and inter-chain correlators (α_y and α_z).

By using the operator identity $S_i^2 = S_i^+ S_i^- - S_i^z + (S_i^z)^2$ we get the sum rule

$$\langle S_j^- S_j^+ \rangle = \langle S_j^+ S_j^- \rangle = \frac{1}{2}, \quad (4)$$

where $\langle S_j^z \rangle = 0$ was used. The decoupling scheme (3) leads to the equation $-\ddot{S}_{\mathbf{q}}^+ = \omega_{\mathbf{q}}^2 S_{\mathbf{q}}^+$ in momentum space. Then we get

$$\chi_{\mathbf{q}}^{+-}(\omega) = -\langle\langle S_{\mathbf{q}}^+; S_{-\mathbf{q}}^- \rangle\rangle_{\omega} = \frac{M_{\mathbf{q}}}{\omega_{\mathbf{q}}^2 - \omega^2} \quad (5)$$

with the dispersion relation

$$\begin{aligned} \omega_{\mathbf{q}}^2 = & \sum_n J_n^2 (1 - \cos(\mathbf{r}_n \mathbf{q})) (1 + 2p_{2\mathbf{r}_n} - 2p_{\mathbf{r}_n}) \\ & - \sum_n J_n^2 (1 - \cos(\mathbf{r}_n \mathbf{q})) (4\cos(\mathbf{r}_n \mathbf{q}) p_{\mathbf{r}_n}) \\ & + \sum_{n \neq m} J_n J_m (1 - \cos(\mathbf{r}_n \mathbf{q})) (4p_{\mathbf{r}_n + \mathbf{r}_m} - 4\cos(\mathbf{r}_m \mathbf{q}) p_{\mathbf{r}_n}) \\ & + 2J_1 J_2 (1 - \cos(q_x)) (3 + 2\cos(q_x)) (p_{(1,0,0)} - p_{(3,0,0)}), \end{aligned} \quad (6)$$

where the following abbreviations are used:

$$\begin{aligned} J_3 = J_{\perp,y}, \quad J_4 = J_{\perp,z}, \\ r_1 = (1, 0, 0), \quad r_2 = (2, 0, 0), \quad r_3 = (0, 1, 0), \quad r_4 = (0, 0, 1), \\ p_{(n,0,0)} = \alpha_x c_{n00}, \quad p_{(m,n,0)} = \alpha_y c_{mn0}, \\ p_{(m,0,n)} = \alpha_z c_{m0n}, \quad p_{(0,n,m)} = (\alpha_y + \alpha_z) c_{0nm} / 2. \end{aligned} \quad (7)$$

Moreover, lattice symmetry is exploited to reduce the number of non-equivalent correlators entering Eq. (6). Expanding $\omega_{\mathbf{q}}$ around $\mathbf{q} = \Gamma = (0, 0, 0)$ we find $\frac{\partial \omega_{\mathbf{q}}}{\partial q_i}|_{\mathbf{q}=0} = v_i$ and $\frac{\partial^2 \omega_{\mathbf{q}}}{2\partial q_i^2}|_{\mathbf{q}=0} = \rho_i$. Here the quantities v_i , $i = x, y, z$, are the spin-wave velocities relevant for AFM J_{\perp} , and ρ_i , $i = x, y, z$, are the spin-stiffness parameters relevant for FM J_{\perp} . The corresponding equations for the spin-wave velocities v_i (Eqs. (A.7), (A.8) and (A.9)) and for the spin stiffnesses ρ_i (Eqs. (A.10), (A.11) and (A.12)) are provided in the Appendix.

The uniform static spin susceptibility is obtained via $\chi_0 = \lim_{\mathbf{q} \rightarrow 0} \chi_{\mathbf{q}}$, $\chi_{\mathbf{q}} = \chi_{\mathbf{q}}(\omega = 0) = \chi_{\mathbf{q}}^{+-}(\omega = 0)/2$. The explicit expression for χ_0 is given in the Appendix, see, Eqs. (A.1), (A.2) (A.3), and (A.4). (Note that finally Eqs. (A.1), (A.2) and (A.3) yield $\chi_0 = \chi_0^{(1)} = \chi_0^{(2)} = \chi_0^{(3)}$, because of the isotropy constraint, see below.) The correlation functions $c_{\mathbf{R}} = \frac{1}{N} \sum_{\mathbf{q}} c_{\mathbf{q}} e^{i\mathbf{q}\mathbf{R}}$ are given by the spectral theorem,⁸⁰

$$c_{\mathbf{q}} = \langle S_{\mathbf{q}}^+ S_{-\mathbf{q}}^- \rangle = \frac{M_{\mathbf{q}}}{2\omega_{\mathbf{q}}} [1 + 2n(\omega_{\mathbf{q}})], \quad (8)$$

where $n(\omega) = (e^{\omega/T} - 1)^{-1}$ is the Bose-Einstein distribution function. In the long-range ordered phase the correlation function $c_{\mathbf{R}}$ is written as^{58,61,68,79}

$$c_{\mathbf{R}} = \frac{1}{N} \sum_{\mathbf{q} \neq \mathbf{Q}} c_{\mathbf{q}} e^{i\mathbf{q}\mathbf{R}} + e^{i\mathbf{Q}\mathbf{R}} C_{\mathbf{Q}}, \quad (9)$$

where $c_{\mathbf{q}}$ is given by Eq. (8). The condensation term $C_{\mathbf{Q}}$, i.e. the long-range part of the correlation functions, is associated with the magnetic wave vector \mathbf{Q} , which describes the magnetically long-range ordered phase. Depending on the sign of $J_{\perp,y}$ and $J_{\perp,z}$ the magnetic wave vector is $\mathbf{Q} = (0, Q_y, Q_z)$, where $Q_y = 0$ ($Q_z = 0$) for FM $J_{\perp,y} < 0$ ($J_{\perp,z} < 0$) and $Q_y = \pi$ ($Q_z = \pi$) for AFM $J_{\perp,y} > 0$ ($J_{\perp,z} > 0$). The order parameter, i.e. the corresponding (sublattice) magnetization M , is connected with the condensation term by the formula $M = \sqrt{3C_{\mathbf{Q}}/2}$. The magnetic correlation length $\xi_{\mathbf{Q}}$ in the paramagnetic regime ($T > T_c$) is obtained by expanding the static susceptibility $\chi_{\mathbf{q}}$ around the magnetic wave-vector \mathbf{Q} , i.e. $\chi_{\mathbf{q}} \sim \chi_{\mathbf{Q}}/(1 + \xi_{\mathbf{Q}}^2(\mathbf{Q} - \mathbf{q})^2)$, see, e.g., Refs. 61, 65, 66, and 68.

Finally we have to make sure that as many equations are provided as unknown quantities are given. Obviously the inverse Fourier transformation of Eq. (8) yields an equation for each spatial spin-spin correlation function appearing in the system of coupled equations that has to be solved numerically. Three more equations are required to determine the vertex parameters α_x , α_y and α_z . One equation is provided by the sum rule Eq. (4), and the remaining two equations are obtained by the isotropy constraint, see, e.g., Refs. 65, 66, and 68, i.e. the static susceptibility $\chi_{\mathbf{q}}$ has to be isotropic in the limit $\mathbf{q} \rightarrow 0$: $\lim_{q_z \rightarrow 0} \chi(q_x = 0, q_y = 0, q_z) = \chi_0^{(1)} = \lim_{q_y \rightarrow 0} \chi(q_x = 0, q_y, q_z = 0) = \chi_0^{(2)}$ and $\lim_{q_x \rightarrow 0} \chi(q_x = 0, q_y = 0, q_z) =$

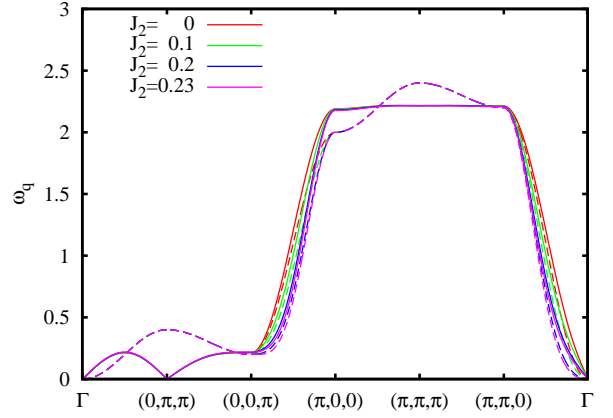


Figure 2. (Color online) Spin-wave dispersion $\omega_{\mathbf{q}}$ as a function of the wave vector \mathbf{q} at zero temperature along several paths through the Brillouin Zone (dashed lines: FM $J_{\perp} = -0.1$; solid lines: AFM $J_{\perp} = 0.1$). Note that in the regions $\Gamma \dots (0, 0, \pi)$ and $(\pi, 0, 0) \dots \Gamma$ all solid as well as all dashed lines coincide.

$\lim_{q_x \rightarrow 0} \chi(q_x, q_y = 0, q_z = 0) = \chi_0^{(3)}$, where analytical expressions for $\chi_0^{(i)}$, $i = 1, 2, 3$, are given in the Appendix, see Eqs. (A.1) - (A.4). Moreover, in the magnetically ordered phase we use the divergence of the static susceptibility $\chi_{\mathbf{Q}}^{-1} = 0$ at the corresponding magnetic wave-vector \mathbf{Q} to calculate the condensation term $C_{\mathbf{Q}}$, see e.g. Refs. 68, 70, and 79. For antiferromagnetic IC ($J_{\perp,y} > 0$ and $J_{\perp,z} > 0$), for instance, the relevant staggered susceptibility $\chi_{(0,\pi,\pi)}$ is given by Eq. (A.5), and the condition for long-range order reads as $\Delta_{(0,\pi,\pi)} = 0$, see Eq. (A.6), which corresponds to the vanishing of the gap in $\omega_{\mathbf{q}}$ at $\mathbf{q} = \mathbf{Q} = (0, \pi, \pi)$.

III. RESULTS

Although, the two ICs $J_{\perp,y}$ and $J_{\perp,z}$ are treated as independent variables in our theory, in what follows we will consider the case with identical ICs in y - and z -direction, i.e. $J_{\perp,y} = J_{\perp,z} = J_{\perp}$. Moreover, we set $J_1 = -1$ and we focus on weak and moderate IC $|J_{\perp}| \leq 1$.

A. Zero-temperature properties

For ferromagnetic ICs J_{\perp} and $0 \leq J_2 < -J_1/4$ the GS is the fully polarized long-range ordered ferromagnetic state, i.e., we have $\langle S_0 S_{\mathbf{R}} \rangle = 1/4$ and the total magnetization is $M = 1/2$ (i.e., the condensation term is $C_{\mathbf{Q}^{FM}} = 1/6$). The corresponding spin-wave dispersion $\omega_{\mathbf{q}}$ is shown in Fig. 2 (dashed lines) for $J_{\perp} = -0.1$ and various values of J_2 . Obviously, the influence of J_2 on the general shape of $\omega_{\mathbf{q}}$ is fairly weak. At the magnetic wave-vector $\mathbf{q} = \mathbf{Q}^{FM} = \mathbf{0}$ (Γ point) there is a quadratic dispersion (i.e., $\omega_{q_i} \propto \rho_i q_i^2$, with $i = x, y, z$), that is typ-

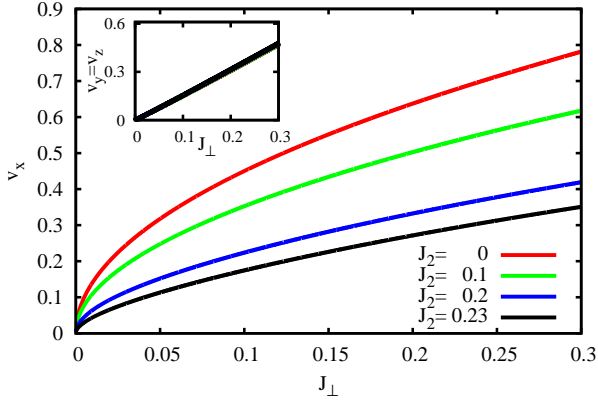


Figure 3. (Color online) GS spin-wave velocities v_x (in-chain, main panel) and $v_y = v_z$ (inter-chain, inset) as a function of the AFM IC $J_\perp > 0$ for different values of the frustrating NNN in-chain coupling J_2 . Note that the curves of the inter-chain velocities in the inset nearly coincide.

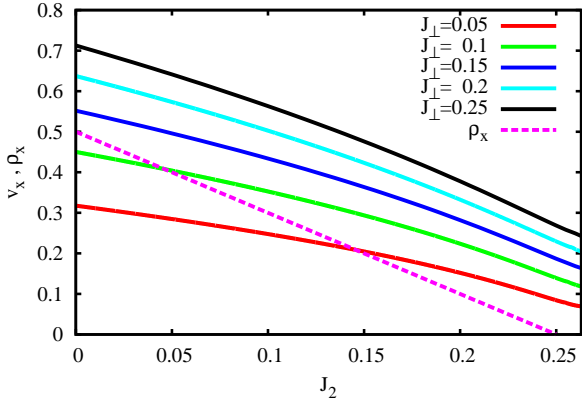


Figure 4. (Color online) GS in-chain spin-wave velocity v_x (solid lines, AFM J_\perp) as well as the in-chain spin stiffness ρ_x (dotted line, FM J_\perp) as a function of the frustration parameter J_2 for different values of the IC J_\perp . Note that ρ_x given by $\rho_x = (|J_1| - 4J_2)/2$ is independent of J_\perp .

ical for ferromagnets. The stiffness parameters, see also Eqs. (A.10) and (A.11), are given by $\rho_x = |J_1 + 4J_2|/2$ (in-chain) and $\rho_\gamma = |J_{\perp,\gamma}|/2$ ($\gamma = y, z$, inter-chain).

In the case of AFM ICs $J_\perp > 0$ the GS is of quantum nature. The corresponding magnetic wave-vector is $Q^{AFM} = (0, \pi, \pi)$. The dispersion is linear for small values of $|\mathbf{q}|$, i.e., the low-lying excitations are determined by the spin-wave velocities v_x and $v_y = v_z$. Again, the influence of J_2 on the general shape of $\omega_{\mathbf{q}}$ is fairly weak, cf. the solid lines in Fig. 2. Since several GS correlation functions enter the expressions for the spin-wave velocities, cf. Eqs. (A.7) and (A.8), no simple expressions can be given. However, it can be seen from these equations that v_x , v_y , and v_z are vanishing in the limit $J_\perp \rightarrow 0^+$ as expected. We show the spin-wave velocities in Figs. 3

and 4. Obviously, the inter-chain spin-wave velocities are almost linear functions in J_\perp , i.e. $v_\gamma \sim aJ_\perp$, $\gamma = y, z$, and their dependence on the frustration parameter J_2 is weak, cf. the inset of Fig. 3. The prefactor a varies between $a = 1.57$ at $J_2 = 0$ and $a = 1.60$ at $J_2 = 0.23$. On the other hand, the in-chain spin-wave velocity v_x exhibits a square-root like dependence on J_\perp , cf. the main panel of Fig. 3. The influence of the in-chain frustration J_2 on v_x (relevant for AFM J_\perp) and ρ_x (relevant for FM J_\perp) is shown in Fig. 4.

The main effect of the frustration consists in a softening of the long-wavelength excitations, i.e. v_x and ρ_x decrease with growing J_2 , where v_x depends on J_\perp and ρ_x is independent of J_\perp . However, in contrast to ρ_x the spin-wave velocity v_x remains finite at the transition point J_2^c , as it is known, e.g., for the square-lattice $J_1 - J_2$ model.^{49–51}

Next we consider the magnetic order parameter M for AFM IC, which is related to the condensation term $C_{\mathbf{Q}}$ at the magnetic wave vector $\mathbf{Q} = \mathbf{Q}^{AFM} = (0, \pi, \pi)$, cf. Sec. II. We show the dependence of M on the IC in Fig. 5. Starting from $M = 1/2$ at $J_\perp = 0$ the order parameter decreases monotonously with increasing J_\perp indicating the role of quantum fluctuations introduced to the system by AFM J_\perp . Moreover, it can be seen from Fig. 5 that the larger J_2 the steeper the decrease of M with growing J_\perp . A more explicit view on the influence of frustration J_2 on M is presented in Fig. 6. As can be expected already from Fig. 5, we have a monotonic decrease of the order parameter with increasing J_2 , i.e. naturally frustration acts against magnetic ordering. The breakdown of the $Q^{AFM} = (0, \pi, \pi)$ long-range order at a critical value J_2^c is indicated by a steep downturn of M . A particular feature is the slight shift of the transition point J_2^c beyond the critical point of isolated chains, $J_2^c = 1/4$, see Fig. 6. Thus we get $J_2^c \approx 0.256$ for $J_\perp = 0.1$ and $J_2^c \approx 0.258$ for $J_\perp = 0.2$. Such a shift of J_2^c to higher values was previously also reported for the two-dimensional case, i.e. $J_{\perp,y} > 0$ and $J_{\perp,z} = 0$, see Ref. 11.

Finally we briefly discuss the uniform static susceptibility χ_0 for AFM J_\perp , see Eq. (A.1). Consistently, χ_0 diverges at $J_\perp = 0$. The inverse uniform susceptibility, $1/\chi_0$, as a function of J_\perp is shown in the inset of Fig. 5. Obviously, $1/\chi_0$ is an almost linear function of J_\perp , and the dependence on the frustration parameter J_2 is weak. A fit according to $\chi_0^{-1} = aJ_\perp$ of the data shown in Fig. 5 yields $a = 12.25, 12.35, 12.56$, and 12.69 for $J_2 = 0, 0.1, 0.2$, and 0.23 , respectively.

B. Finite-temperature properties

For the very existence of magnetic long-range order in an isotropic Heisenberg spin system at finite temperatures a 3D exchange pattern is necessary,⁷⁷ i.e., finite ICs, $J_{\perp,y} \neq 0$ and $J_{\perp,z} \neq 0$ are required. Again in this section we consider the special case of $J_{\perp,y} = J_{\perp,z} = J_\perp$. We mention that RGM data for the physical quantities

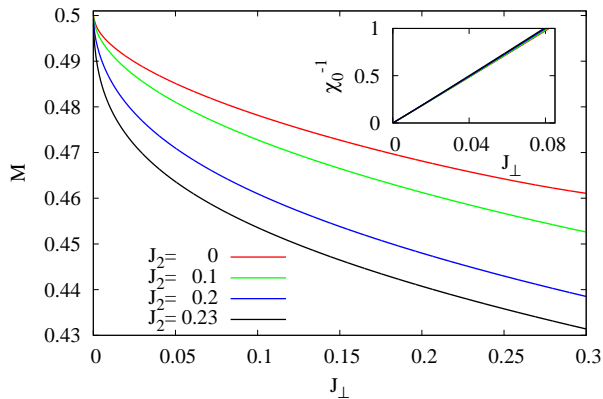


Figure 5. (Color online) GS magnetic order parameter M (main panel) and inverse uniform susceptibility χ_0^{-1} (inset) as a function of the AFM IC J_\perp for different values of the frustrating NNN in-chain coupling J_2 . Note that the curves of the inverse uniform susceptibility in the inset practically coincide.

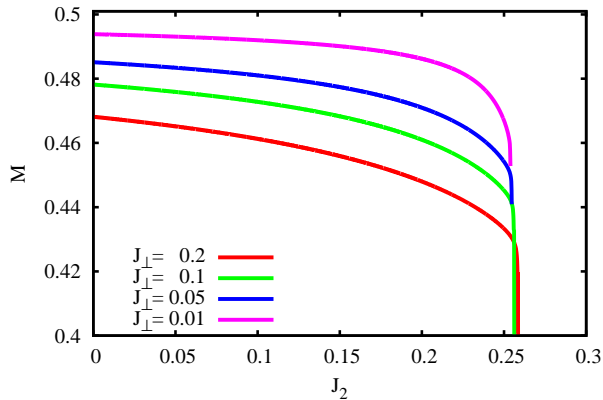


Figure 6. (Color online) GS magnetic order parameter M as a function of the frustrating NNN in-chain coupling J_2 for different values of AFM IC $J_\perp > 0$.

at arbitrary sets of J_2 , $J_{\perp,y}$ and $J_{\perp,z}$ are available upon request.

1. Order parameters, critical temperatures and spin-spin correlation functions

In Fig. 7 we show some typical temperature profiles of the order parameter calculated for $J_\perp = \pm 0.1$ and various values of frustrating J_2 . In accordance with previous studies on quasi-two-dimensional unfrustrated spin systems^{78,79} we find that for $J_2 = 0$ the transition temperature T_c is larger if AFM interactions are present. If $J_2 > 0$ the transition temperature is a result of a subtle interplay of frustration J_2 and IC J_\perp , since these parameters influence T_c in an opposite direction. An illustration

of the influence of J_2 and J_\perp on T_c is provided in Figs. 8 and 9. From Fig. 8 (main panel) it is obvious that the slope of the $T_c(J_\perp)$ curve is largest at $J_\perp \sim 0$. Moreover, following the trend observed at $J_2 = 0$ we find that T_c for AFM $J_\perp \gtrsim 0.1$ is larger than T_c for corresponding FM IC irrespective of the strength of frustration. As we can see from Fig. 9 (main panel) the reduction of T_c due to frustration is moderate as long as J_2 is not too close to the critical strength of frustration J_2^c , where the FM GS ordering along the chains breaks down. Only as approaching J_2^c there is a drastic downturn of T_c , cf. also Ref. 70.

It is useful to compare the calculated critical temperatures with the Curie-Weiss temperature Θ_{CW} given for the model at hand by $\Theta_{CW} = -\frac{1}{2}(J_1 + J_2 + J_{\perp,y} + J_{\perp,z})$, where $J_1 = -1$ (FM) and $J_2 \geq 0$ (AFM). The absolute value of Θ_{CW} can be considered as a measure for the strength of the exchange interactions. Thus, in ordinary unfrustrated 3D magnets it determines the magnitude of the critical temperature T_c . The ratio $f = |\Theta_{CW}/T_c|$ is often considered as the degree of frustration see, e.g., Refs. 82–84. In conventional 3D ferro- and antiferromagnets this ratio is of the order of unity, whereas $f \gtrsim 5$ indicates a suppression of magnetic ordering. One may expect that also for unfrustrated or weakly frustrated quasi-2D (quasi-1D) systems in the limit of small inter-layer (inter-chain) coupling the parameter f can be large. We show f in the insets of Figs. 8 and 9. Indeed from Fig. 8 we notice that for $|J_\perp| < 0.05$ the ratio f increases drastically. Thus, even for $J_2 = 0$ we find $f > 5$ at $J_\perp < 0.022$. The role of the frustrating coupling J_2 is illustrated in Fig. 9. It is obvious, that the influence of J_2 is weak in a wide range of J_2 values. Only as approaching the critical frustration J_2^c there is a tremendous increase of f beyond $f > 10$. We may conclude that the magnitude of the frustration parameter is a result of a subtle interplay of J_\perp and J_2 , and, a large value of f does not unambiguously indicate frustration.

The order-disorder transition is also evident in the spin-spin correlation functions $\langle \mathbf{S}_0 \mathbf{S}_{\mathbf{R}} \rangle$, see Figs. 10 and 11. Thus, for small $|J_\perp|$ the inter-chain correlations $\langle \mathbf{S}_0 \mathbf{S}_{\mathbf{R}} \rangle$, $\mathbf{R} = (0, 0, n)$, become very small at $T > T_c$, whereas the correlations along the chain direction, $\langle \mathbf{S}_0 \mathbf{S}_{\mathbf{R}} \rangle$, $\mathbf{R} = (n, 0, 0)$, remain pretty large at $T \gtrsim T_c$ indicating the magnetic short-range order along the chains in the paramagnetic phase. The effect of in-chain frustration J_2 is also visible by comparing the green lines in Figs. 10 and 11.

2. Correlation length and uniform static susceptibility

The correlation length, shown in Fig. 12 for the unfrustrated case, illustrates clearly the different behavior of the inter- and in-chain correlations, if J_\perp is noticeably smaller than J_1 . While the inter-chain correlation length drops down very rapidly towards one lattice spacing for $T \gtrsim T_c$, the in-chain correlation length remains quite

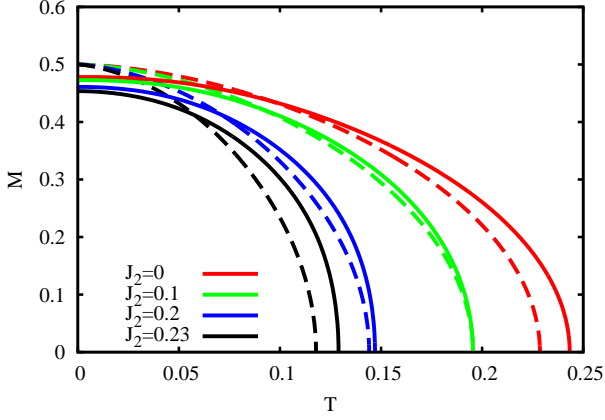


Figure 7. (Color online) Temperature dependence of the magnetic order parameter M for AFM $J_{\perp} = +0.1$ (solid lines) and FM $J_{\perp} = -0.1$ (dashed lines) and various values of the frustrating in-chain coupling J_2 .

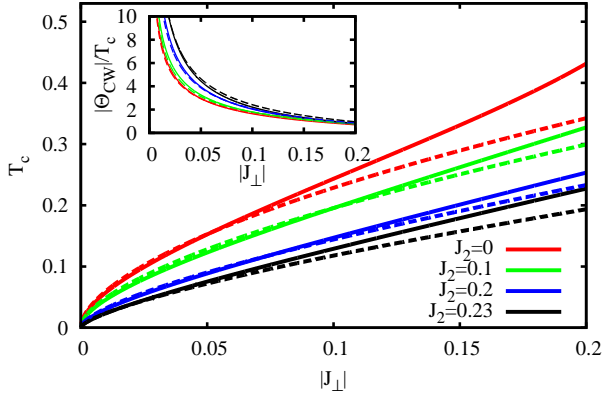


Figure 8. (Color online) Main panel: Critical temperature T_c as a function of the IC J_{\perp} (FM - dashed; AFM - solid) for several values of the frustrating in-chain coupling $J_2 > 0$. Inset: Ratio $f = |\Theta_{CW}/T_c|$ of the Curie-Weiss temperature $\Theta_{CW} = -\frac{1}{2}(J_1 + J_2 + 2J_{\perp})$ and the critical temperature T_c .

large in a wider region above T_c indicating the 1D nature of the magnetic behavior above the transition. The role of the in-chain frustration on the correlation lengths becomes evident by comparing Figs. 12 and 13. For strong frustration $J_2 = 0.2$ used for the presentation in Fig. 13 the correlation lengths form a narrow bundle, i.e., the differences between the in-chain and the inter-chain correlation lengths become much smaller compared to the case $J_2 = 0$, since the in-chain correlations on longer separations are substantially diminished by frustration.

The temperature dependence of the susceptibility χ_0 presented in Fig. 14 exhibits the typical behavior of antiferromagnets (main panel) and ferromagnets (left inset). The effect of frustration is evident for both FM and AFM J_{\perp} . For FM J_{\perp} the overall shape of the curve is very similar for different J_2 . However, there is a noticeable shift

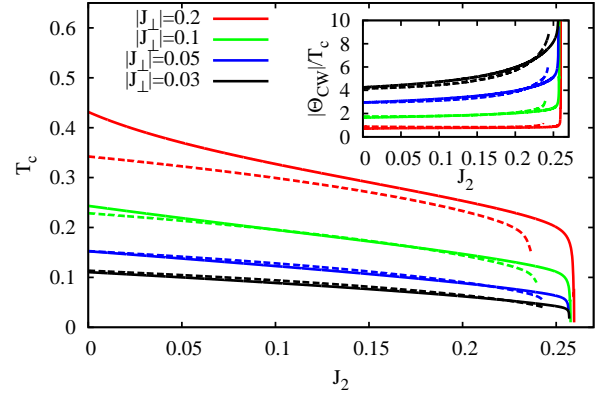


Figure 9. (Color online) Main panel: Critical temperature T_c as a function of the frustrating in-chain coupling $J_2 > 0$ for several values of the IC J_{\perp} (FM - dashed; AFM - solid). Inset: Ratio $f = |\Theta_{CW}/T_c|$ of the Curie-Weiss temperature $\Theta_{CW} = -\frac{1}{2}(J_1 + J_2 + 2J_{\perp})$ and the critical temperature T_c .

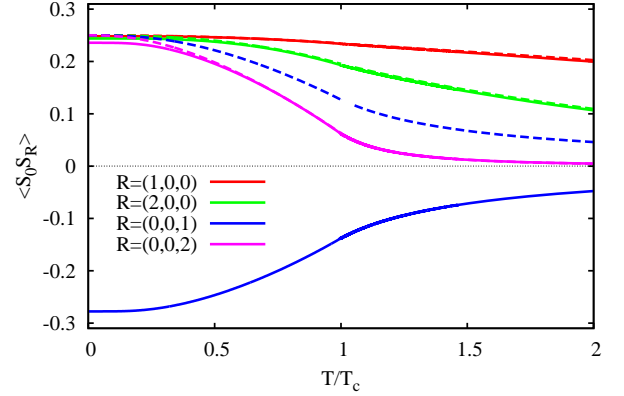


Figure 10. (Color online) Several spin-spin correlation functions as a function of the normalized temperature T/T_c for the IC $|J_{\perp}| = 0.1$ (AFM - solid; FM - dashed) and for $J_2 = 0$. Note that the solid and dashed lines are very close to each other (except for $\mathbf{R} = (0, 0, 1)$).

towards higher values of T/T_c as increasing J_2 . For AFM J_{\perp} the shape of $\chi_0(T)$ above T_c is affected by J_2 . For the IC of $J_{\perp} = 0.1$ used in Fig. 14 the critical temperature T_c is small and there is a broad maximum in χ_0 noticeably above T_c related to the inter-chain antiferromagnetic correlations. By increasing J_2 the position of this maximum is shifted towards larger values of T/T_c : it is at $T/T_c = 1.05$ for $J_2 = 0$ and at $T/T_c = 1.23$ for $J_2 = 0.2$, see the right inset in Fig. 14. On the other hand, below T_c the influence of J_2 on the $\chi_0(T/T_c)$ curves is very weak. The influence of J_{\perp} on the temperature profile of χ_0 for AFM IC is depicted in Fig. 15. Except the influence of the IC on the critical temperature discussed in Sec. III B 1 the strength of the AFM IC has also a strong influence on the magnitude of the uniform susceptibility

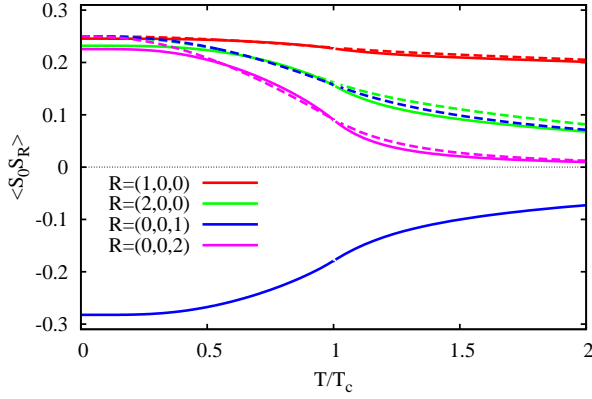


Figure 11. (Color online) Several spin-spin correlation functions as a function of the normalized temperature T/T_c for the IC $|J_\perp| = 0.1$ (AFM solid; FM dashed) and for $J_2 = 0.2$. Note that the solid and dashed lines are very close to each other (except for $\mathbf{R} = (0, 0, 1)$).

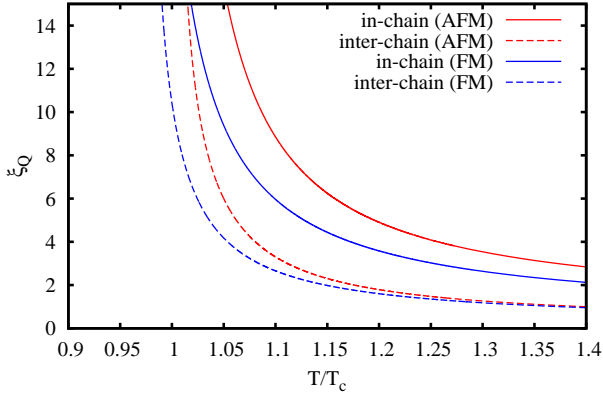


Figure 12. (Color online) Correlation length ξ_Q as a function of the normalized temperature T/T_c for $J_2 = 0$ (FM $J_\perp = -0.2$ - blue; AFM $J_\perp = 0.2$ - red; in-chain correlation length - solid, inter-chain correlation length - dashed).

at the transition point, $\chi_0(T_c)$, in case of weak IC. That is related to the behavior of χ_0 in the limit $J_\perp \rightarrow 0+$, where we have $T_c \rightarrow 0$ and $\chi_0(T_c) \rightarrow \infty$. Thus, as lowering J_\perp from moderate values to zero, $\chi_0(T_c)$ increases drastically. Below T_c the AFM IC leads to a characteristic downturn of χ_0 , cf. Fig. 15.

3. Excitation spectrum and specific heat

Finally we consider the temperature dependence of energetic quantities such as the specific heat $C_V(T)$, the spin-wave velocities v_γ (for AFM J_\perp) and the spin stiffnesses ρ_γ (for FM J_\perp), where $\gamma = x, y, z$. Let us start with a few remarks with respect to the comparison between the RGM and the standard random-phase approx-

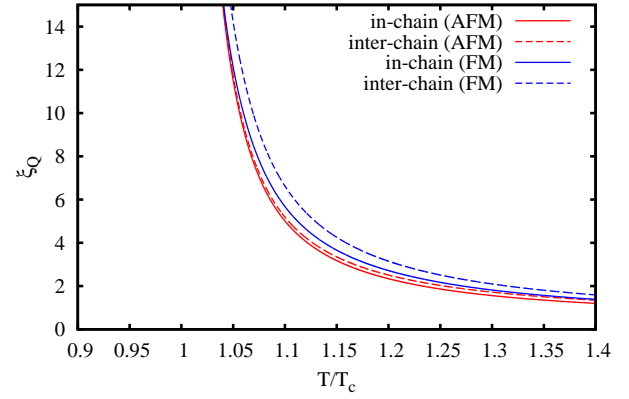


Figure 13. (Color online) Correlation length ξ_Q as a function of the normalized temperature T/T_c for $J_2 = 0.2$ (FM $J_\perp = -0.2$ - blue; AFM $J_\perp = +0.2$ - red; in-chain correlation length - solid, inter-chain correlation length - dashed).

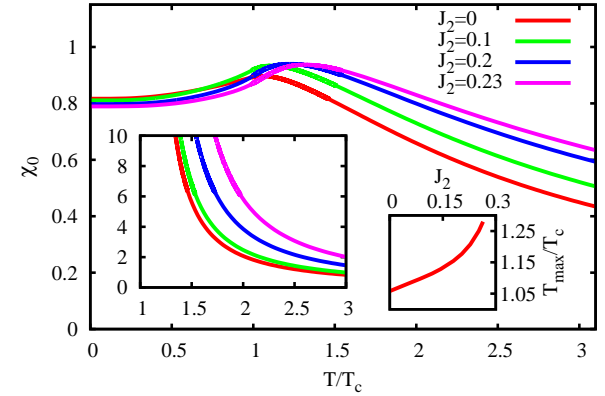


Figure 14. (Color online) Main panel: Uniform static susceptibility χ_0 as a function of the normalized temperature T/T_c for several values of the frustrating in-chain coupling J_2 and AFM $J_\perp = 0.1$. Left inset: Uniform susceptibility χ_0 as a function of the normalized temperature T/T_c for several values of the frustrating in-chain coupling J_2 and FM $J_\perp = -0.1$. Right inset: Position of the maximum of the uniform susceptibility χ_0 , T_{\max}/T_c as a function of J_2 for AFM $J_\perp = 0.1$.

imation (RPA), see, e.g., Refs. 70, 80, 85–88. The spin-wave excitation energies obtained within the framework of the RGM, see Eq. (6), show a temperature renormalization that is wavelength dependent and proportional to the correlation functions. Thus, as an example, the existence of spin-wave excitations does not imply a finite magnetization. By contrast, within the RPA, the temperature renormalization of the excitations is independent of the wavelength and proportional to the magnetization, see, e.g., Refs. 80 and 81. Moreover, the RPA fails in describing magnetic excitations and magnetic short-range order for $T > T_c$, reflected, e.g., in the specific heat.^{80,81,87}

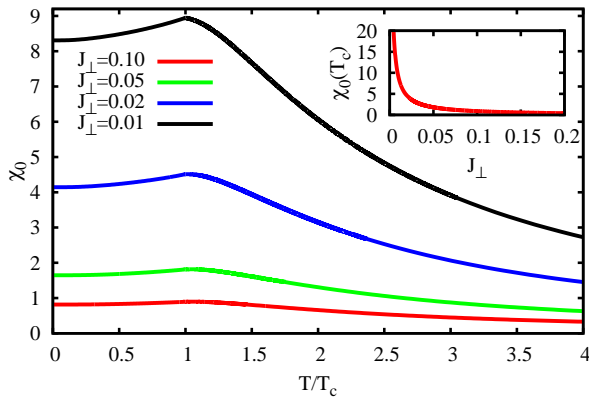


Figure 15. (Color online) Main panel: Uniform susceptibility χ_0 as a function of the normalized temperature T/T_c for several values of the AFM IC J_\perp and $J_2 = 0$. Inset: The value of the uniform susceptibility at the transition temperature, $\chi_0(T_c)$ as a function of the AFM IC J_\perp for $J_2 = 0$.

According to the above discussion on the temperature dependence of the excitation spectrum, the RGM is appropriate to provide also information on the temperature dependence of v_γ and ρ_γ ($\gamma = x, y, z$), cf. Ref. 70. We show the in-chain and inter-chain spin-wave velocities (relevant for AFM IC) in Figs. 16 and 17, respectively, and of the corresponding stiffnesses (relevant for FM IC) in Figs. 18 and 19, respectively. Typically, the stiffness and the spin-wave velocity decrease with increasing temperature indicating a softening of spin excitations at $T > 0$, cf. Refs. 70, 71, 89–93. Interestingly, an opposite trend of the temperature influence on v_x and ρ_x can emerge as increasing J_2 towards the transition point J_2^c . That is in accordance with recent studies on other frustrated ferromagnets^{70,71} and could therefore be interpreted as a signature of frustration in (anti-)ferromagnets. The temperature dependence of ρ_x at $J_2 = 0.23$, i.e. very close to the transition point J_2^c , is somehow special, since it is first decreasing and then increasing with temperature.

As discussed already in Sec. IIIB 1 the degree of frustration often is related to the ratio of the Curie-Weiss temperature Θ_{CW} and the transition temperature T_c , i.e. to $f = |\Theta_{CW}/T_c|$. We also mentioned in Sec. IIIB 1 that a large value of f does not unambiguously signalize frustration, since small values of J_\perp also may lead to large values of f even without any frustrating couplings. Hence, the unusual temperature dependence of the spin-wave velocity and the stiffness discussed above can be understood as another criterion to detect frustration.

The temperature dependence of the specific heat C_V is shown in Fig. 20 for $J_2 = 0$ and two values of J_\perp . The $C_V(T)$ curves show the characteristic cusp-like behavior at the transition temperature T_c indicating the second-order phase transition. For very small values of J_\perp above the cusp a separate broad maximum emerges

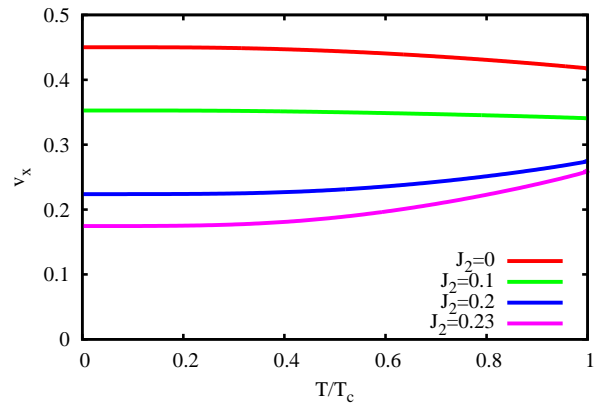


Figure 16. (Color online) In-chain spin-wave velocity v_x as a function of the normalized temperature T/T_c for AFM IC $J_\perp = 0.1$ and for different values of the frustrating NNN in-chain coupling J_2 .

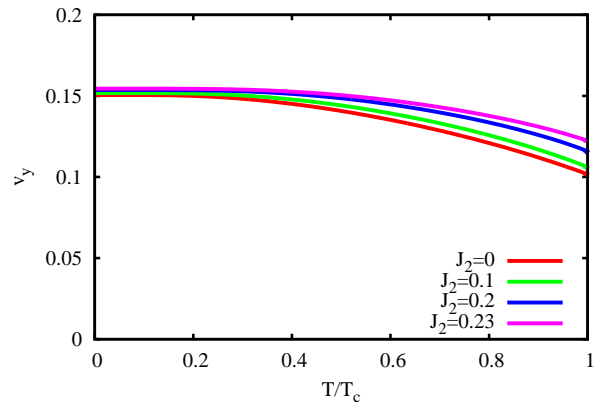


Figure 17. (Color online) Inter-chain spin-wave velocity $v_y = v_z$ as a function of the normalized temperature T/T_c for AFM IC $J_\perp = 0.1$ and for different values of the frustrating NNN in-chain coupling J_2 .

which is related to the in-chain spin-spin correlations, i.e., the position of this maximum is mainly determined by the in-chain exchange parameters, cf. Ref. 9.

IV. SUMMARY

In our paper we investigate coupled frustrated spin-1/2 J_1 - J_2 Heisenberg chains with FM NN exchange J_1 and AFM NNN exchange J_2 . We consider FM as well as AFM inter-chain couplings (ICs) $J_{\perp,y}$ and $J_{\perp,z}$ corresponding to the axis perpendicular to the chain. We focus on the regime of weak and moderate values of J_2 , such that the in-chain spin-spin correlations are predominantly FM. We use the rotation-invariant Green's function method (RGM) to calculate thermodynamic quantities, such as the (sublattice) magnetization (magnetic

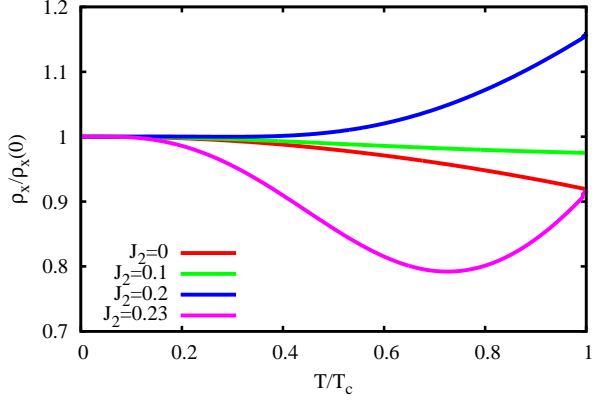


Figure 18. (Color online) In-chain spin stiffness ρ_x scaled by its value at $T = 0$ as a function of the normalized temperature T/T_c for FM IC $J_\perp = -0.1$ for different values of the frustrating NNN in-chain coupling J_2 .

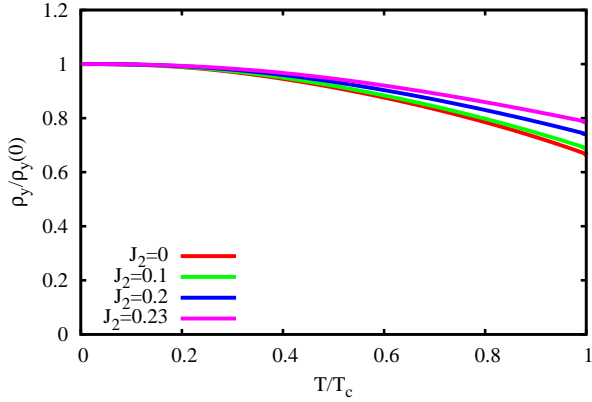


Figure 19. (Color online) Inter-chain spin stiffness $\rho_y = \rho_z$ scaled by its value at $T = 0$ as a function of the normalized temperature T/T_c for FM IC $J_\perp = -0.1$ for different values of the frustrating NNN in-chain coupling J_2 .

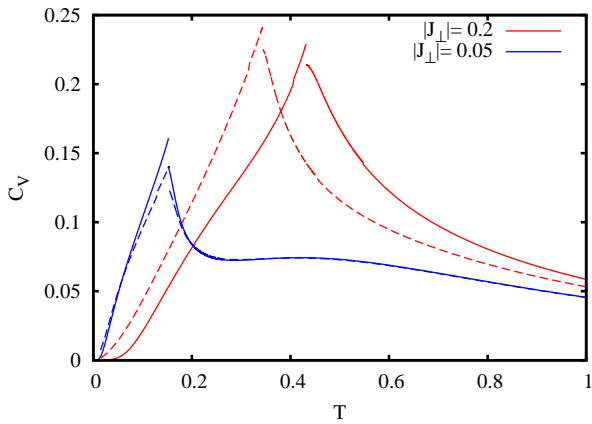


Figure 20. (Color online) Temperature dependence of the specific heat C_V for various values of J_\perp and $J_2 = 0$ (dashed lines: FM J_\perp ; solid lines: AFM J_\perp).

order parameter) M , the critical temperature T_c , the correlation functions $\langle \mathbf{S}_0 \mathbf{S}_{\mathbf{R}} \rangle$, the uniform static susceptibility χ_0 , the correlation length $\xi_{\mathbf{Q}}$, the specific heat C_V , the spin stiffnesses as well as the spin-wave velocities. The RGM goes one step beyond the random-phase approximation (RPA). As a result, several shortcomings of the RPA, see, e.g., Refs. 80, 81, 85, 86, and 88, such as the artificial equality of the critical temperatures T_c for FM and AFM couplings or the failure in describing the paramagnetic phase at $T > T_c$, can be overcome. As approaching the ground-state transition point to the helical in-chain phase at $J_2 \sim |J_1|/4$, the thermodynamic properties are strongly influenced by the frustration. Thus, there is a drastic decrease of T_c as $J_2 \rightarrow |J_1|/4$. Moreover, the temperature profile of the in-chain spin stiffness ρ_x (for FM IC) or the in-chain spin-wave velocity (for AFM IC) may exhibit an increase with T instead of the ordinary decrease.

The present investigations are focused on theoretical aspects, and we consider the simplest case of perpendicular ICs. Although, there are a few materials corresponding to perpendicular ICs, e.g., LiVCuO_4 and $\text{Li(Na)Cu}_2\text{O}_2$ ^{30,31,34,47}, in real magnetic J_1 - J_2 compounds typically the ICs are more sophisticated than those we consider in our paper, see, e.g., Ref. 54.

ACKNOWLEDGMENTS

We thank S.-L. Drechsler and O. Derzhko for fruitful discussions.

Appendix: Analytical Expressions

In this section we provide analytical expressions of the uniform susceptibility χ_0 , the staggered susceptibility $\chi_{\mathbf{Q}=(0,\pi,\pi)}$, the spin-wave stiffnesses ρ_i and the spin-wave velocities v_i ($i = x, y, z$), which enter the equations given in Sec. II.

Static susceptibility:

$$\lim_{q_z \rightarrow 0} \chi(q_x = 0, q_y = 0, q_z) = \chi_0^{(1)} = -\frac{2c_{001}}{-4J_1p_{001} + 4J_1p_{101} - 4J_{\perp,y}p_{001} + 4J_{\perp,y}p_{011} - 6J_{\perp,z}p_{001} + 2J_{\perp,z}p_{002} - 4J_2p_{001} + 4J_2p_{201} + J_{\perp,z}}, \quad (\text{A.1})$$

$$\lim_{q_y \rightarrow 0} \chi(q_x = 0, q_y, q_z = 0) = \chi_0^{(2)} = -\frac{2c_{010}}{-4J_1p_{010} + 4J_1p_{110} - 6J_{\perp,y}p_{010} + 2J_{\perp,y}p_{020} - 4J_{\perp,z}p_{010} + 4J_{\perp,z}p_{011} - 4J_2p_{010} + 4J_2p_{210} + J_{\perp,y}}, \quad (\text{A.2})$$

$$\lim_{q_x \rightarrow 0} \chi(q_x, q_y = 0, q_z = 0) = \chi_0^{(3)} = \frac{2J_1c_{100} + 8J_2c_{200}}{\Delta_0^{(3)}}, \quad (\text{A.3})$$

$$\Delta_0^{(3)} = J_1^2(6p_{100} - 2p_{200} - 1) + 2J_1(2J_{\perp,y}(p_{100} - p_{110}) + 2J_{\perp,z}p_{100} - 2J_{\perp,z}p_{101} - 3J_2p_{100} + 8J_2p_{200} - 5J_2p_{300}) + 4J_2(4(J_{\perp,y}p_{200} - J_{\perp,y}p_{210} + J_{\perp,z}p_{200} - J_{\perp,z}p_{201}) + J_2(6p_{200} - 2p_{400} - 1)), \quad (\text{A.4})$$

$$\chi_{(0,\pi,\pi)} = -\frac{2(J_{\perp,y}c_{010} + J_{\perp,z}c_{001})}{\Delta_{(0,\pi,\pi)}}, \quad (\text{A.5})$$

$$\begin{aligned} \Delta_{(0,\pi,\pi)} &= 4J_{\perp,y}(-J_1p_{010} + J_1p_{110} + J_{\perp,z}(p_{001} + p_{010} + 2p_{011}) - J_2p_{010} + J_2p_{210}) \\ &\quad + J_{\perp,z}(-4J_1p_{001} + 4J_1p_{101} + 2J_{\perp,z}p_{001} + 2J_{\perp,z}p_{002} - 4J_2p_{001} + 4J_2p_{201} + J_{\perp,z}) \\ &\quad + J_{\perp,y}^2(2p_{010} + 2p_{020} + 1). \end{aligned} \quad (\text{A.6})$$

Spin-wave velocities:

$$\begin{aligned} v_x^2 &= J_1^2 \left(-3p_{100} + p_{200} + \frac{1}{2} \right) \\ &\quad + J_1(2J_{\perp,y}(p_{110} - p_{100}) - 2J_{\perp,z}p_{100} + 2J_{\perp,z}p_{101} + 3J_2p_{100} - 8J_2p_{200} + 5J_2p_{300}) \\ &\quad + 2J_2(-4J_{\perp,y}p_{200} + 4J_{\perp,y}p_{210} - 4J_{\perp,z}p_{200} + 4J_{\perp,z}p_{201} - 6J_2p_{200} + 2J_2p_{400} + J_2), \end{aligned} \quad (\text{A.7})$$

$$\begin{aligned} 2v_y^2/J_{\perp,y} &= -4J_1p_{010} + 4J_1p_{110} - 6J_{\perp,y}p_{010} + 2J_{\perp,y}p_{020} - 4J_{\perp,z}p_{010} \\ &\quad + 4J_{\perp,z}p_{011} - 4J_2p_{010} + 4J_2p_{210} + J_{\perp,y}, \end{aligned} \quad (\text{A.8})$$

$$\begin{aligned} 2v_z^2/J_{\perp,z} &= -4J_1p_{001} + 4J_1p_{101} - 4J_{\perp,y}p_{001} + 4J_{\perp,y}p_{011} - 6J_{\perp,z}p_{001} \\ &\quad + 2J_{\perp,z}p_{002} - 4J_2p_{001} + 4J_2p_{201} + J_{\perp,z}. \end{aligned} \quad (\text{A.9})$$

Spin stiffnesses:

$$\begin{aligned} 24\rho_x^2 &= J_1^2(30p_{100} - 2p_{200} - 1) + 16J_2(4(J_{\perp,y}p_{200} - J_{\perp,y}p_{210} + J_{\perp,z}p_{200} - J_{\perp,z}p_{201}) + J_2(30p_{200} - 2p_{400} - 1)) \\ &\quad + 2J_1(2J_{\perp,y}(p_{100} - p_{110}) + 2J_{\perp,z}p_{100} - 2J_{\perp,z}p_{101} + 3J_2p_{100} + 8J_2p_{200} - 17J_2p_{300}), \end{aligned} \quad (\text{A.10})$$

$$\begin{aligned} 36\rho_y^2 &= -6J_{\perp,y}(J_1(p_{110} - p_{010}) - J_{\perp,z}p_{010} + J_{\perp,z}p_{011} - J_2p_{010} + J_2p_{210}) \\ &\quad - J_{\perp,y}^2(3(p_{020} - 15p_{010}) + \frac{3}{2}), \end{aligned} \quad (\text{A.11})$$

$$\begin{aligned} 36\rho_z^2 &= -6J_{\perp,z}(J_1(p_{101} - p_{001}) - J_{\perp,y}p_{001} + J_{\perp,y}p_{011} - J_2p_{001} + J_2p_{201}) \\ &\quad - J_{\perp,z}^2(3(p_{002} - 15p_{001}) + \frac{3}{2}). \end{aligned} \quad (\text{A.12})$$

¹ W. Selke, Z.f.Physik B: Condensed Matter **27**, 81 (1977).

² H.P. Bader and R. Schilling, Phys. Rev. B **19**, 3556 (1979).

- ³ T. Hamada, J. Kane, S. Nakagawa, and Y. Natsume, J. Phys. Soc. Jpn. **57**, 1891 (1988); **58**, 3869 (1989).
- ⁴ A. V. Chubukov, Phys. Rev. B **44**, 4693(R) (1991).
- ⁵ D.V. Dmitriev, V.Ya. Krivnov, and A.A. Ovchinnikov, Phys. Rev. B **56**, 5985 (1997).
- ⁶ D. V. Dmitriev, V. Ya. Krivnov, and J. Richter Phys. Rev. B **75**, 014424 (2007).
- ⁷ T. Vekua, A. Honecker, H.-J. Mikeska, and F. Heidrich-Meisner, Phys. Rev. B **76**, 174420 (2007).
- ⁸ T. Hikihara, L. Kecke, T. Momoi, and A. Furusaki, Phys. Rev. B **78**, 144404 (2008).
- ⁹ M. Härtel, J. Richter, D. Ihle, and S.-L. Drechsler, Phys. Rev. B **78**, 174412 (2008).
- ¹⁰ J. Sudan, A. Lüscher, and A. M. Läuchli, Phys. Rev. B **80**, 140402 (2009).
- ¹¹ R. Zinke, S.-L. Drechsler, and J. Richter, Phys. Rev. B **79**, 094425 (2009).
- ¹² R. Shindou and T. Momoi, Phys. Rev. B **80**, 064410 (2009).
- ¹³ J. Sirker, Phys. Rev. B **81**, 014419 (2010).
- ¹⁴ D. V. Dmitriev and V. Ya. Krivnov, Phys. Rev. B **82**, 054407 (2010).
- ¹⁵ M. E. Zhitomirsky, and H. Tsunetsugu, Europhysics Letters **92**, 37001 (2010).
- ¹⁶ M. Arlego, F. Heidrich-Meisner, A. Honecker, G. Rossini, and T. Vekua, Phys. Rev. B **84**, 224409 (2011).
- ¹⁷ A. Lavarello, G. Roux, and N. Laflorencie, Phys. Rev. B **84**, 144407 (2011).
- ¹⁸ M. Chen and C. D. Hu, Phys. Rev. B **84**, 094433 (2011).
- ¹⁹ M. Härtel, J. Richter, D. Ihle, J. Schnack, and S.-L. Drechsler, Phys. Rev. B **84**, 104411 (2011).
- ²⁰ M. Härtel, J. Richter, and D. Ihle, Phys. Rev. B **83**, 214412 (2011).
- ²¹ A. V. Syromyatnikov, Phys. Rev. B **86**, 014423 (2012).
- ²² C. Lee, Jia Liu, M.-H. Whangbo, H.-J. Koo, R. K. Kremer, and A. Simon, Phys. Rev. B **86**, 060407(R) (2012).
- ²³ D. Bimla, K. Brijesh, and V. P. Ramesh, Europhysics Letters **100**, 27003 (2012).
- ²⁴ D. V. Dmitriev and V. Ya. Krivnov, Phys. Rev. B **86**, 134407 (2012).
- ²⁵ A. Smerald and N. Shannon, Phys. Rev. B **88**, 184430 (2013).
- ²⁶ M. Sato, T. Hikihara, and T. Momoi, Phys. Rev. Lett. **110**, 077206 (2013).
- ²⁷ O. A. Starykh, and L. Balents, Phys. Rev. B **89**, 104407 (2014).
- ²⁸ K. Manoranjan, P. Aslam, and G. S. Zoltán, arXiv:1507.03720 (2015).
- ²⁹ O. Hiroaki, arXiv:1506.06891 (2015).
- ³⁰ A. A. Gippius, E. N. Morozova, A. S. Moskvina, A. V. Zalessky, A. A. Bush, M. Baenitz, H. Rosner, and S.-L. Drechsler, Phys. Rev. B **70**, 020406 (2004).
- ³¹ M. Enderle, C. Mukherjee, B. Fak, R.K. Kremer, J.-M. Broto, H. Rosner, S.-L. Drechsler, J. Richter, J. Málek, A. Prokofiev, W. Assmus, S. Pujol, J.-L. Raggazoni, H. Rakato, M. Rheinstädter, and H.M. Ronnow, Europhys. Lett. **70**, 237 (2005).
- ³² S.-L. Drechsler, O. Volkova, A.N. Vasiliev, N. Tristan, J. Richter, M. Schmitt, H. Rosner, J. Málek, R. Klingeler, A.A. Zvyagin, and B. Büchner, Phys. Rev. Lett. **98**, 077202 (2007).
- ³³ S.-L. Drechsler, J. Richter, R. Kuzian, J. Málek, N. Tristan, B. Büchner, A.S. Moskvina, A.A. Gippius, A. Vasiliev, O. Volkova, A. Prokofiev, H. Rakato, J.-M. Broto, W. Schnelle, M. Schmitt, A. Ormeci, C. Loison, and H. Rosner, J. Magn. Magn. Mater. **316**, 306 (2007).
- ³⁴ N. Büttgen, H.-A. Krug von Nidda, L. E. Svistov, L. A. Prozorova, A. Prokofiev, and W. Aßmus, Phys. Rev. B **76**, 014440 (2007).
- ³⁵ S. E. Dutton, M. Kumar, M. Mourigal, Z. G. Soos, J.-J. Wen, C. L. Broholm, N. H. Andersen, Q. Huang, M. Zbiri, R. Toft-Petersen, and R. J. Cava, Phys. Rev. Lett. **108**, 187206 (2012).
- ³⁶ M. Pregelj, A. Zorko, O. Zaharko, D. Arčon, M. Komelj, A. D. Hillier, and H. Berger, Phys. Rev. Lett. **109**, 227202 (2012).
- ³⁷ A. Saul and G. Radtke, Phys. Rev. B **89**, 104414 (2014).
- ³⁸ A. Fennell, V. Y. Pomjakushin, A. Uldry, B. Delley, B. Prevost, A. Desilets-Benoit, A. D. Bianchi, R. I. Bewley, B. R. Hansen, T. Klimczuk, R. J. Cava, and M. Kenzelmann, Phys. Rev. B **89**, 224511 (2014).
- ³⁹ K. Nawa, Y. Okamoto, A. Matsuo, K. Kindo, and Y. Kitahara, J. Phys. Soc. Jpn. **83**, 103702 (2014).
- ⁴⁰ N. Büttgen, K. Nawa, T. Fujita, M. Hagiwara, P. Kuhns, A. Prokofiev, A. P. Reyes, L. E. Svistov, K. Yoshimura, and M. Takigawa, Phys. Rev. B **90**, 134401 (2014).
- ⁴¹ L. A. Prozorova, S. S. Sosin, L. E. Svistov, N. Büttgen, J. B. Kemper, A. P. Reyes, S. Riggs, A. Prokofiev, and O. A. Petrenko, Phys. Rev. B **91**, 174410 (2015).
- ⁴² B. Willenberg, M. Schäpers, A.U.B. Wolter, S.-L. Drechsler, M. Reehuis, J.-U. Hoffmann, B. Büchner, A.J. Studer, K.C. Rule, B. Ouladdiaf, S. Süllo, and S. Nishimoto, Phys. Rev. Lett. **116**, 047202 (2016).
- ⁴³ F. Weickert, M. Jaime, N. Scott Harrison, B. L. Leitmäe, A. Heinmaa, I. Stern, R. Janson, O. Berger, H. Rosner, and A. A. Tsirlin, arXiv:1602.01632 (2016).
- ⁴⁴ K. Caslin, R. K. Kremer, F. S. Razavi, M. Hanfland, K. Syassen, E. E. Gordon, and M.-H. Whangbo, Phys. Rev. B **93**, 022301 (2016).
- ⁴⁵ M. Matsuda, K. Ohoyama, and M. Ohashi, J. Phys. Soc. Jpn. **68**, 269 (1999).
- ⁴⁶ H. F. Fong, B. Keimer, J. W. Lynn, A. Hayashi, and R. J. Cava, Phys. Rev. B **59**, 6873 (1999).
- ⁴⁷ S.-L. Drechsler, J. Richter, A.A. Gippius, A. Vasiliev, A.A. Bush, A.S. Moskvina, J. Málek, Yu. Prots, W. Schnelle and H. Rosner, EPL (Europhysics Letters) **73**, 83 (2006).
- ⁴⁸ R. O. Kuzian, S. Nishimoto, S.-L. Drechsler, J. Málek, S. Johnston, Jeroen van den Brink, M. Schmitt, H. Rosner, M. Matsuda, K. Oka, H. Yamaguchi, and T. Ito, Phys. Rev. Lett. **109**, 117207 (2012).
- ⁴⁹ S. Chakravarty, B.I. Halperin, D.R. Nelson, Phys. Rev. B **39**, 2344 (1989).
- ⁵⁰ H.J. Schulz and T.A.L. Ziman, Europhys. Lett. **18**, 355 (1992); H.J. Schulz, T.A.L. Ziman, and D. Poilblanc, J. Phys. I **6**, 675 (1996).
- ⁵¹ J. Richter and J. Schulenburg, Eur. Phys. J. B **73**, 117 (2010).
- ⁵² H. T. Ueda and K. Totsuka, Phys. Rev. B **80**, 014417 (2009).
- ⁵³ S. Nishimoto, S.-L. Drechsler, R.O. Kuzian, J. van den Brink, J. Richter, W.E.A. Lorenz, Y. Skourski, R. Klingeler, and B. Büchner, Phys. Rev. Lett. **107**, 097201 (2011).
- ⁵⁴ S. Nishimoto, S.-L. Drechsler, R. Kuzian, J. Richter, and J. van den Brink, Phys. Rev. B **92**, 214415 (2015).
- ⁵⁵ Z. Z. Du, H. M. Liu, Y. L. Xie, Q. H. Wang, and J.-M. Liu Phys. Rev. B **94**, 134416 (2016).
- ⁵⁶ J. Kondo and K. Yamaji, Prog. Theor. Phys. **47**, 807 (1972).

- ⁵⁷ E. Rhodes and S. Scales, Phys. Rev. B **8**, 1994 (1973).
- ⁵⁸ H. Shimahara and S. Takada, J. Phys. Soc. Jpn. **60**, 2394 (1991).
- ⁵⁹ F. Suzuki, N. Shibata, and C. Ishii, J. Phys. Soc. Jpn. **63**, 1539 (1994).
- ⁶⁰ A. F. Barabanov, and V. M. Berezovskii, J. Phys. Soc. Jpn. **63**, 3974 (1994); Phys. Lett. A **186**, 175 (1994); Zh. Eksp. Teor. Fiz. **106**, 1156 (1994) [JETP **79**, 627 (1994)].
- ⁶¹ S. Winterfeldt and D. Ihle, Phys. Rev. B **56**, 5535 (1997).
- ⁶² L. Siurakshina, D. Ihle, and R. Hayn, Phys. Rev. B **64**, 104406 (2001).
- ⁶³ B.H. Bernhard, B. Canals, and C. Lacroix, Phys. Rev. B **66**, 104424 (2002).
- ⁶⁴ D. Schmalfuß, J. Richter, and D. Ihle, Phys. Rev. B **70**, 184412 (2004).
- ⁶⁵ I. J. Junger, D. Ihle, and J. Richter, Phys. Rev. B **72**, 064454 (2005).
- ⁶⁶ D. Schmalfuß, J. Richter, and D. Ihle, Phys. Rev. B **72**, 224405 (2005).
- ⁶⁷ D. Schmalfuß, R. Darradi, J. Richter, J. Schulenburg, and D. Ihle, Phys. Rev. Lett. **97**, 157201 (2006).
- ⁶⁸ M. Härtel, J. Richter, O. Götze, D. Ihle, and S.-L. Drechsler, Phys. Rev. B **87**, 054412 (2013).
- ⁶⁹ M. Härtel, J. Richter, D. Ihle, and S.-L. Drechsler, Phys. Rev. B **81**, 174421 (2010).
- ⁷⁰ P. Müller, J. Richter, A. Hauser and D. Ihle. Eur. Phys. J. B **88**, 159 (2015).
- ⁷¹ A.N. Ignatenko, A. A. Katanin, and V. Yu. Irkhin, JETP Lett. **97**, 209 (2013).
- ⁷² H.J. Schulz, Phys. Rev. Lett. **77**, 2790 (1996).
- ⁷³ V. Yu. Irkhin and A. A. Katanin Phys. Rev. B **61**, 6757 (2000).
- ⁷⁴ M. Bocquet, Phys. Rev. B **65**, 184415 (2002).
- ⁷⁵ Zvyagin, A. A., and Drechsler, S.-L., Phys. Rev. B **78**, 014429 (2008).
- ⁷⁶ J. Richter, P. Müller, A. Lohmann, and H.-J. Schmidt, Physics Procedia **75**, 813 (2015).
- ⁷⁷ N.D. Mermin and H. Wagner, *Phys. Rev. Lett.* **17**, 1133, (1966).
- ⁷⁸ J. Oitmaa and Weihong Zheng, J. Phys.: Condens. Matter **16**, 8653 (2004).
- ⁷⁹ I. Juhász Junger, D. Ihle, and J. Richter, Phys. Rev. B **80**, 064425 (2009).
- ⁸⁰ S. V. Tyablikov, *Methods in the Quantum Theory of Magnetism* (Plenum, New York, 1967).
- ⁸¹ W. Gasser, E. Heiner, and K. Elk, *Greensche Funktionen in Festkörper- und Vielteilchenphysik*. WILEY-VCH, 2001.
- ⁸² L. Balents, Nature **464**, 199 (2010).
- ⁸³ A. G. Mihailov, A. Mailman, A. Assoud, C. M. Robertson, B. Wolf, M. Lang, and R. T. Oakley J. Am. Chem. Soc. **138**, 10738 (2016).
- ⁸⁴ A. M. Hallas, A. Z. Sharma, Y. Cai, T. J. Munsie, M. N. Wilson, M. Tachibana, C. R. Wiebe, and G. M. Luke, arXiv:1607.08657.
- ⁸⁵ A. Du and G.Z. Wei, J. Magn. Magn. Mater. **137**, 343 (1994).
- ⁸⁶ P. Froebrich and P.J. Kuntz, Physics Reports **432**, 223 (2006).
- ⁸⁷ I. Juhász Junger, D. Ihle, L. Bogacz, and W. Janke, Phys. Rev. B **77**, 174411 (2008).
- ⁸⁸ M.R. Pantic, D.V. Kapor, S.M. Radošević, and P. Mali, Solid State Comm. **182**, 55 (2014).
- ⁸⁹ S.W. Lovesey, J. Phys. C: Solid State Phys. **10**, L455 (1977).
- ⁹⁰ Shih-Jye Sun and Hsiu-Hau Lin, Eur. Phys. J. B **49**, 403 (2006).
- ⁹¹ I.A. Fomin, ZhETF, **78**, 2392 (1980) (English translation - JETP **51**, 1203, (1980)).
- ⁹² Y.M. Bunkov, in *Progress in Low Temperature Physics*, Vol. **14**, p. 69 ed. W.P. Halperin (North Holland, San Diego 1995).
- ⁹³ Jin An, Chang-De Gong, and Hai-Qing Li, J. Phys.: Condens. Matter **13**, 115 (2001).